

Statistical properties of contact vectors

A. Kabakçioğlu¹, I. Kanter², M. Vendruscolo³, and E. Domany¹

¹*Department of Physics of Complex Systems, Weizmann Institute of Science, Rehovot 76100, Israel*

²*Department of Physics, Bar Ilan University, 52900 Ramat Gan, Israel*

³*Oxford Centre for Molecular Sciences, Central Chemistry Laboratory
University of Oxford, South Parks Road, OX1 3QH Oxford UK*

Abstract

We study the statistical properties of *contact vectors*, a construct to characterize a protein's structure. The contact vector of an N -residue protein is a list of N integers n_i , representing the number of residues in contact with residue i . We study analytically (at mean-field level) and numerically the amount of structural information contained in a contact vector. Analytical calculations reveal that a large variance in the contact numbers reduces the degeneracy of the mapping between contact vectors and structures. Exact enumeration for lengths up to $N = 16$ on the three dimensional cubic lattice indicates that the growth rate of number of contact vectors as a function of N is only 3% less than that for contact maps. In particular, for compact structures we present numerical evidence that, practically, each contact vector corresponds to only a handful of structures. We discuss how this information can be used for better structure prediction.

I. Introduction

The protein folding problem has been the subject of extensive research in the last decade and although much has been learned a satisfactory understanding of the phenomenon has

not been reached yet [1–3]. The physical approach to the problem is to consider the native state of a protein as the ground-state of a Hamiltonian which acts on sequence space and summarizes the inter-residue and residue-solvent interactions [1,2,4]. Recently it was shown that there are several cases for which there is no possible choice of pairwise contact interactions between residues that suffices to pin down the native state even for a single protein [5,6]. This conclusion is supported by molecular dynamics studies [7] and lattice models [8] on residue-solvent interactions, where many-body forces are shown, or can be deduced to be, as relevant as two-body forces. To get around this failure of the two-body Hamiltonian approach while retaining a coarse-grained description (as opposed to, say, an all-atom one, including water [9]), we need to introduce new terms at the residue level, to bias the optimization procedure towards the true minima.

It is widely accepted that hydrophobicity is the force driving the folding process [10]. At the individual residue level, hydrophobicity is correlated with the solvent-exposed surface area in the native state [11]. In addition, as reported below, a statistical analysis of the native structures deposited in the Protein Data Bank (PDB) [12]) reveals a good correlation (coefficient of correlation 0.8) between the solvent-hidden surface area per residue and the number of inter-residue contacts per residue in the native state. We therefore propose the following two-step procedure for predicting the native state of a protein. First, a reasonably accurate prediction of the exposed surface area in the native fold is made on the basis of sequence information [11]. Second, this information is translated into a prediction of the number of native contacts of each residue, e.g. to a predicted native *contact vector*. Even if this scheme will turn out to be insufficient to perform a successful prediction, it opens the possibility to confine the search for the native fold to a small portion of the conformational space. The question then becomes “How many folded configurations are there, consistent with a given set of contact numbers ?” And, for that matter, “Is such a contact-number representation of the protein structure degenerate at all ?” The rest of this paper addresses these questions.

II. Contact maps versus contact vectors

The contact map (CM) [13] of a protein of N amino-acids is a symmetric binary matrix C of size $N \times N$, such that $C_{ij} = 1$ when the i^{th} and the j^{th} amino-acids of the sequence are neighbors, with some suitable definition of “neighborhoodness” (e.g., a common construct is to threshold the pairwise distance matrix for the C_α atoms [5]). The CM has proven to be a convenient encoding of the 3-dimensional native fold: 1. The native backbone conformation can be reproduced to within $\sim 1.5 \text{ \AA}$ average uncertainty (the same as most X-ray data) [14], 2. It allows for an efficient search of the configuration space, since large conformational changes can be obtained by minor modifications of the CM [15]. Within such minimalistic framework one hopes to gain new insight to the protein-folding problem since it is amenable to different physical and mathematical tools. For instance, the following Hamiltonian acting on the contact map space has been extensively used in the past [16–19] :

$$H = \sum_{ij} w(a_i, a_j) C_{ij} , \quad (1)$$

where $w(\alpha, \beta)$ is one of the 210 energy parameters representing the contact energy between the amino-acid types α and β . Unfortunately, this formulation has limited predictive power. For example, given a large enough set of sequences and decoys (obtained by threading) from the PDB, no set of $w(\alpha, \beta)$ exists, for which H has its ground-states at the native-folds [6]. This is in accordance with the recent studies on the nature of the hydrophobic interaction [7,8], whose conclusion is that many-body interactions are of the same order of magnitude as two-body interactions.

One possible way to improve the Hamiltonian in Eq. (1) is to include an energy penalty for deviations from the native-contacts:

$$H = (1 - \lambda) \sum_{ij} w(a_i, a_j) C_{ij} + \lambda \sum_i (n_i - n_i^{nat})^2 \quad (2)$$

where we define a “contact vector” (CV) \vec{n} of rank N , which is the sum of the entries of the CM on each row (or column) (see Fig.(1)) :

$$n_i = \sum_j C_{ij} . \quad (3)$$

Contact vectors have already been studied in the context of protein folding [20–28]. We note in particular that the second term in Eq. (2) resembles a hydrophobic term introduced previously [29] and studied in Ref. [30], with the difference that there the desired number of contacts of residue i is determined by its species. Here instead we assume the knowledge of n_i^{nat} , the correct number of contacts of residue i in the native structure. Hence the second term in Eq. (2) carries the same spirit as the Go model [31]. In this work we are interested in studying the statistical properties of contact vectors. For our more general purpose, it would seem inconsistent to use Eq. (2) to predict the native structure of a protein, as we bias the Hamiltonian towards the minimum by using information which is not accessible to us before we actually solve the problem. However, unlike in the Go model, the information required here about the native state (the *number* of contacts for each residue) is modest, and, most crucially, can be predicted. Learning algorithms have been recently developed, which are trained on known structures to predict the surface exposure of the amino-acids in the native fold [11,32]. Since the hydrophobic effect is driving the folding process [10], it is natural to expect that an accurate prediction of the solvent exposed surface of each residue in the folded state may lead to prediction of the correct native structure. To bridge the gap between the exposed-surface information and the CV defined above, we performed an analysis on a representative set of proteins from the PDB database. We found a linear correlation with a coefficient of correlation of 0.8 between the solvent *hidden* surface area of a residue and the number of amino-acids it is in contact with (see Fig.(2)). Therefore, in future work we expect to replace the n_i^{nat} term in Eq. (2) by $n_i^{predicted}$, thereby breaking the causality loop which is a characteristic of Go-like models. Another reason to study the model of Eq. (2) is that a related kind of Hamiltonian has been recently proved to be useful to determine the structure of nearly-native protein conformations [33]. In that study, n_i represent the number of *native* contacts formed by residue i in the contact map C . Also in that case, it was found that a large variance in n_i (see below) implies a low degeneracy in

mapping between contact vectors and three-dimensional conformations.

In studying Eq. (2), first we tried to use a set of contact energy parameters $w(a_i, a_j)$, found earlier by an optimization process, using Eq. (2) with $\lambda = 0$. This attempt failed to assign the minimal energy to the native state for any choice of λ . However, an optimization of $w(\alpha, \beta)$ over the known structures by using the Hamiltonian in Eq. (2) with $\lambda \neq 0$ may, perhaps, successfully identify the native state. We will investigate this possibility in the future.

The Hamiltonian (2), with $\lambda = 1$, fails to identify the native fold. This statement means that it is possible to find conformations which on the one hand are very different from the native one and, on the other, each amino-acid has exactly the correct number of neighbors, that is the same number of neighbors as in the native state. This result was first found by Ejtehadi *et al.* [22] by exact enumeration of all the compact conformations on a $3 \times 3 \times 3$ cubic lattice. For actual proteins, an example is given in Fig. 3 in the case of protein CI2 (PDB code 2ci2), where the CMs of the native fold and of another conformation are superimposed. These two conformations have identical CVs. At first glance, it would seem unlikely to find two compact configurations where each residue has exactly the same number of neighboring residues in contact. On the other hand, the cautious reader will attribute this degeneracy to the loss of information (from $N(N - 1)/2$ binary variables to N integers of size $\leq N$) associated with going from a given CM to its corresponding CV via Eq. (3). Quantifying the resulting degeneracy is a non-trivial problem. The next section is an analytical attempt in this direction.

III. An analytical approach

We ask the following question: “How many contact maps exist for a given contact vector \vec{n} ?” In fact, we should be counting, for a given \vec{n} , only the *physical* CM that are consistent with it. A physical CM [29,14] is one for which a perfectly matching chain configuration can be found. There is, however, no known analytical selection rule for the physical CMs among all symmetric and traceless $N \times N$ matrices; therefore in our analytic study we will

consider all binary symmetric matrices. This is essentially the mean-field treatment of the problem, since in the limit of infinite dimensions, all the constraints on the CM, except being symmetric with zero trace, will be relaxed. For any finite dimension we overestimate the degeneracy - the number of physical CMs scales exponentially, as e^N , whereas the number of possible CMs scales as e^{N^2} [13].

The formal expression for the number of symmetric, traceless binary matrices consistent with a given vector, \vec{n} , is

$$d(\vec{n}) = \sum_{\{x_{ij}\}} \prod_{i=1}^{i>j} \prod_{i=1}^N \delta_{(\sum_j x_{ij}), n_i} . \quad (4)$$

The sum over $x_{ij} = 0, 1$ represents a trace over all binary matrices, and the constraint $i > j$ ensures symmetry and zero trace. In order to perform the summation, we rewrite the Kronecker δ as a discrete Fourier sum:

$$\begin{aligned} d(\vec{n}) &= \sum_{\{c_{ij}\}} \prod_{i=1}^{i>j} \prod_{i=1}^N \left[\frac{1}{N} \sum_{k=0}^{N-1} e^{i2\pi \frac{k}{N} (\sum_j x_{ij} - n_i)} \right] \\ &= \frac{1}{N^N} \sum_{k_1=0}^{N-1} \sum_{k_2=0}^{N-1} \dots \sum_{k_N=0}^{N-1} \left(\sum_{\{x_{ij}\}}^{i>j} e^{i\frac{2\pi}{N} \sum_i k_i (\sum_j x_{ij} - n_i)} \right) . \end{aligned} \quad (5)$$

Scaling k_i by N , approximate the sums by integrals. Then, evaluate the trace over the matrix elements, paying special attention to $x_{ij} = x_{ji}$ and $x_{ii} = 0$:

$$\begin{aligned} d(\vec{n}) &= \int_0^1 dk_1 dk_2 \dots dk_N \left(\sum_{\{x_{ij}\}}^{i>j} e^{i2\pi \sum_i k_i (\sum_j x_{ij} - n_i)} \right) \\ &= 2^{N(N-1)/2} \int_0^1 dk_1 dk_2 \dots dk_N e^{-i2\pi \sum_i k_i [(N-1)/2 - n_i]} \prod_{i>j} \cos [\pi (k_i + k_j)] . \end{aligned} \quad (6)$$

The integral can now be evaluated around its saddle points, $k_i = 1/2$ and $k_i = 0, 1$, which contribute equally. After we set $k_i = 1/2 + q_i$ and assume N is divisible by 4, we obtain

$$\simeq 2^{N(N-1)/2} 2 \int_{-1/2}^{1/2} dq_1 dq_2 \dots dq_N e^{-i2\pi \sum_i q_i [(N-1)/2 - n_i] - (\pi^2/2) [N \sum_i q_i^2 + (\sum_i q_i)^2]} . \quad (7)$$

The last square term in the exponent can be eliminated by a Hubbard- transformation after rescaling q_i by \sqrt{N} and defining $\eta_i = n_i - (N-1)/2$:

$$d(\vec{n}) \simeq 2^{N(N-1)/2} \sqrt{\frac{2}{\pi}} \int_{-1/2}^{1/2} dq_1 dq_2 \dots dq_N \int_{-\infty}^{\infty} dy e^{-y^2/2 + i\pi y \sum_i q_i + i2\pi \sum_i \eta_i q_i - N\pi^2/2 \sum_i q_i^2} ,$$

which finally simplifies to yield

$$d(\vec{n}) \simeq \frac{2^{N^2/2}}{(N/\pi)^{N/2} \sqrt{N}} e^{-2\sigma_\eta^2 - \bar{\eta}^2}, \quad (8)$$

where $\bar{\eta}$ and σ_η are the average and the standard deviation of $\eta_i = (n_i - N/2)$. This is a mean-field estimate of how the degeneracy of a CV scales with respect to the statistical properties of the CV. The leading behavior is clearly far from being realistic, since the degeneracy should scale at most as z^N for some $z < z_{CM}$ ($\ln(z_{CM})$ is 0.83 in 2d [13] and 1.32 in 3d as calculated here). Eq. (8) further suggests that the maximally degenerate CV with a fixed average number of contacts has $\sigma_\eta = 0$, i.e., all the amino-acids have equal number of contacts, whereas an unbiased sample of CVs will be dominated by those vectors with a typical standard deviation of $\sigma_\eta \simeq \sqrt{N}$. The mean-field message is that the degeneracy is a decreasing function of σ_η , i.e., variation in contact number is desirable for low degeneracy. In the next section, we argue that this is true away from the saddle point as well.

IV. Finite connectivity : Graph counting

In the previous section, we allowed for the number of contacts to take any value between 0 and N . In reality, and also in lattice models, the number of contacts is of order unity. Therefore, it is desirable to have an estimate of the degeneracy of such CVs. Once again, we consider all traceless, symmetric, binary $N \times N$ matrices. We first observe that every such matrix encodes a unique graph with N vertices, a vertex pair being connected if the corresponding matrix element is 1. Symmetry ensures that the graph is undirected. We can ensure chain connectivity (but not the graph being physical!) by freezing connections on the first off-diagonal; if we choose to relax these “backbone connections”, the remaining graph need not be connected.

The degeneracy of a CV, can then be approximated by the number of graphs with N vertices and given connectivities. We imagine the vertices from 1 to N with corresponding number of legs sticking out of each and we ask in how many ways these legs can be connected such that none will be left out (the total number of legs is an even number). Eq. (9)

follows immediately if one imagines connecting pairs of legs sequentially (the numerator) and remembering that legs coming out of the same vertex are interchangeable (denominator).

Let's assume we allow the entries of the CV to be one of $0, 1, \dots, n$, $n \ll N$, and the composition given by $\{p_0, p_1, \dots, p_n\}$, $p_i N \equiv N_i$ being the number of amino acids with i contacts. The average number of contacts is $\sum_i i p_i \equiv c$. The corresponding number of graphs reads

$$d(N, \{p_i\}) = \frac{(cN - 1)!!}{(0!)^{N_0} (1!)^{N_1} \dots (n!)^{N_n}} . \quad (9)$$

(The only difference with the usual Feynman diagram counting is the missing $N!$ in the denominator: our vertices are distinguishable since they correspond to the amino-acids labelled by their sequence number.)

Note that this expression is an approximation to the number of symmetric traceless CMs, since diagrams with small loops involving one vertex, as well as with more than one line connecting the same two vertices *are* counted in Eq. (9), even though they do not correspond to any CMs. However, corrections due to excluding such diagrams do not change the scaling with N . Applying Stirling's formula to Eq. (9),

$$d(N, \{p_i\}) \simeq \exp \left[\frac{cN}{2} \ln N + N \left(\frac{c}{2} \ln c - 1 - \sum p_n \ln(n!) \right) \right] . \quad (10)$$

The leading order is now $z_F^{N \ln N}$ with $z_F = e^{c/2}$. Better estimations require taking into consideration the spatial correlations in the contact numbers due to the underlying one-dimensional chain. Our next task is to find the compositions with the minimum and maximum degeneracy. The leading order in Eq. (10) depends only on the total number of contacts, so it is sensible to confine the search into the subspace of CVs with a fixed average connectivity. We then extremize the next order term with respect to $\{p_i\}$, subject to the constraints $\sum p_m = 1$ and $\sum m p_m = c$ to find which distribution of contacts allows for the better "designability" (i.e., less degeneracy). Fig.(4) shows the choice of $\{p_i\}$ with maximum/minimum degeneracy obtained numerically, as a function of the average contact number, c (maximum number of non-backbone contacts, n , is chosen to be 4 as for the cubic lattice). As read from the

graphs, the highly degenerate scenario is when the number of contacts for each residue is minimally away from the average, and vice versa for the low degeneracy. Even though here we deal with low connectivity $n_i \ll N$, whereas in the previous section we had $n_i \sim N$, the result obtained here is the same as there - low degeneracy goes in parallel with maximal variation in contact number.

One application of this principle is an order of magnitude estimation for the “optimal” length for a protein. Consider a necklace model of the protein, each residue represented by a sphere of fixed radius, and the necklace itself folded into a large compact sphere, where compactness is imposed as a necessary condition for stability. Then, maximal contact number fluctuation is attained when the number of buried residues equals the number of residues on the surface. From this purely geometric construction, one can estimate an “ideal” chain size: Let the radii of the individual residues be unity, and the radius of the protein be R . Assuming hcp-like packing, each residue occupies a volume of $v = 4\sqrt{2}(\text{unit})^3$, and those on the surface cover, roughly, $a = 4(\text{unit})^2$ of surface area. Then, if N is the number of residues, we have $vN = 4\pi R^3/3$ and $aN/2 = 4\pi R^2$, which yields $N \sim 450$.

V. Numerical results

To compare the analytical findings presented above with numerical simulations, we performed several exact enumeration studies on the square and the cubic lattices. Therefore, in this section, we deal with *physical* CMs and contact vectors, i.e., those generated by self-avoiding walks in two and three dimensions. In each analysis, we kept a record of the distinct CMs we encountered and the corresponding CVs. Our first observation is that, the number of distinct CVs for a given size N scales exponentially with N :

$$N_{cv} \sim e^{a_{cv}N} .$$

For given N , the number of CVs, CMs, and self-avoiding walks increase in the given order. Yet, it is interesting that the growth rate $a_{cv} = 1.28 \pm 0.01$ is only about 3% less than the corresponding rate $a_{cm} = 1.32 \pm 0.01$ for the CMs in three dimensions (see Fig.(5), and

also [13]). The discrepancy between the mean-field analytical calculations and the exact enumeration results points to the fact that the finite dimensionality and the correlations between contacts due to the underlying one-dimensional chain (i.e. working with physical CMs and CVs) are crucial.

The almost identical growth rates is in accordance with our next analysis on the compact configurations on a 6×6 square lattice (see [34]): Considering all the Hamiltonian walks inside a 6×6 square, we identified the number of walks that correspond to each CV and found that the number of CVs with degeneracy d drops more or less exponentially with d (see Fig.(6)). In fact, more than 96% of all the contact vectors have degeneracy $d \leq 6$, although it is possible to find a vector with 69 Hamiltonian walks mapped on it (not shown in Fig.(6)). The degeneracy gets even smaller in the case of a compact but less than perfect packing, in our case when the 6×6 square is mostly filled with a 32-residue chain: introduced vacancies (especially when in the core) “label” some of the residues with otherwise identical contact number. Rearrangement of the core, where all the residues have identical number of contacts, is the dominant mechanism of degeneracy. Hence, it gets more difficult to find conformations with the same CV, once this degeneracy is lifted by the vacancies. In this case, for practically all the CVs we have $d \leq 5$. In three dimensions, for the system sizes within reach, practically all the residues are on the surface. Therefore, we have not extended this analysis to such case.

VI. Conclusion

Existing and future prediction methods for the accessible surface area of individual residues can be adopted to predict the number of native contacts of each amino acid of a given protein. This prediction can then be used for an efficient search of the native contact map (and the corresponding conformation) in a dramatically reduced configuration space. The prerequisite of such a program is to be able to identify different folds consistent with a given set of contact numbers for each residue. We investigated at the mean-field level the partition of the configuration space (or rather the contact map space) into degeneracy

classes labelled by the CVs. The average degeneracy predicted by the analytical calculations disagrees with the numerical findings, indicating that the finite dimensionality and the correlations induced by the underlying one-dimensional chain are crucial even for a qualitatively satisfactory result. We did find, already at the mean-field level, that the increasing the fluctuations in the native contact-numbers reduces the contact vectors' degeneracy. This finding is also supported by another analytical calculation, valid in a different regime, where the average contact number is $O(1)$.

We further investigated by exact enumeration the degeneracy spectrum of CVs for self-avoiding walks on the square and the cubic lattice. We found that for compact self-avoiding walks the CM and the CV representations carry nearly the same amount of information. This is an encouraging result, for an accurate enough prediction of solvent exposed surface areas in the native state may then be used to reduce the search space sufficiently, so that within the limited set of remaining candidate CMs a simple pairwise interaction potential may suffice to single out the native fold of the protein. In addition, we performed exact enumeration over all SAWs of $N \leq 16$ steps in three dimension, and found that the number of CVs grows exponentially with the protein length, with a prefactor only a few percent smaller than that for the CMs. The slow exponential growth of the average degeneracy of the CVs is largely overestimated by our mean-field calculations. Further analytical and numerical research is certainly called for. We also observed that for *compact* configurations, CV \rightarrow CM mapping is practically one-to-few. The Hamiltonian in Eq. (1), therefore, may still be promising if the pairwise interactions are optimized within the context of a (even roughly) predicted CV.

A. K. acknowledges many useful discussions with G. Getz and A. Punnoose and is also grateful to the Bilkent University Physics Department for their hospitality during his visit. This work was partially supported by grants from the US-Israel Binational Science Foundation (BSF) and the Minerva Foundation. I. Kanter thanks the Einstein Center for Theoretical Physics for partial support.

REFERENCES

- [1] A. Sali, E. I. Shakhnovich and M. Karplus Nature, **369**, 248 (1994).
- [2] V.S. Pande, A. Yu. Grosberg and T. Tanaka, Rev. Mod. Phys. **72**, 259 (2000).
- [3] D. Baker, Nature **405**, 39 (2000).
- [4] T. Lazaridis and M. Karplus, Curr. Op. Struct. Biol. **10**, 139 (2000).
- [5] M. Vendruscolo and E. Domany, J. Chem. Phys **109**, 11101 (1998).
- [6] M. Vendruscolo, R. Najmanovich and E. Domany, Proteins **38**, 134 (2000).
- [7] F. Bruguè, S.L. Fornili, G.G. Malenkov, M.B. Palma-Vittorelli and M.U. Palma, Chem. Phys. Lett. **254**, 283 (1996), and references therein.
- [8] P. De Los Rios and Guido Caldarelli, Phys. Rev. E **62**, 8449 (2000).
- [9] Y. Duan and P. A. Kollman, Science **282**, 740 (1998).
- [10] K. A. Dill, S. Bromberg, K. M. Fiebig, D. P. Yee, P. D. Thomas and H. S. Chan, Protein Sci. **4**, 561 (1995).
- [11] B. Rost and C. Sander, Proteins **20**, 216 (1994).
- [12] H. M. Berman *et al*, Nucleic Acids Res. **28**, 235 (2000).
- [13] M. Vendruscolo, B. Subramanian, I. Kanter, E. Domany and J. Lebowitz Phys. Rev. E **59**, 977 (1999).
- [14] M. Vendruscolo, E. Kussell and E. Domany, Folding and Design **2**, 295 (1997).
- [15] M. Vendruscolo and E. Domany, Folding and Design **3**, 329 (1998).
- [16] K. S. Dill *et al.*, Protein Sci. **4**, 561 (1995).
- [17] J. Skolnick *et al.*, Protein Sci. **6**, 676 (1997).
- [18] E. I. Shakhnovich, Curr. Opin. Struct. Biol. **7** 29 (1997).

- [19] S. Miyazawa and R. L. Jernigan, J. Mol. Biol. **256**, 623 (1996).
- [20] S. Saitoh, T. Nakai and K. Nishikawa, Proteins **15**, 191 (1994).
- [21] M. Skorobogatiy, H. Guo and M. J. Zuckermann Macromolecules **30**, 3403 (1997).
- [22] M. R. Ejtehadi *et al*, Phys. Rev. E **57**, 3298 (1998).
- [23] H. Li, C. Tang and N. S. Wingreen, Proc. Natl. Acad. Sci. USA **95**, 4987 (1998).
- [24] M.-H. Hao and H. A. Scheraga, Physica A **244**, 124 (1999).
- [25] A. F. Pereira de Araujo, Proc. Natl. Acad. Sci. USA **96**, 12482 (1999).
- [26] M. R. Ejtehadi, N. Hamedani and V. Shahrezaei, Phys. Rev. Lett. **82**, 4723 (1999).
- [27] V. Shahrezaei, N. Hamedani and M. R. Ejtehadi, Phys. Rev. E **60**, 4629 (1999).
- [28] V. Shahrezaei and M. R. Ejtehadi, J. Chem. Phys. **113**, 6437 (2000).
- [29] L. Mirny and E. Domany, Proteins **26**, 391 (1996).
- [30] K. Park, M. Vendruscolo and E. Domany, Proteins, **40**, 237 (2000).
- [31] N. Go, Ann. Rev. Biophys. Bioeng. **12**, 182 (1983).
- [32] P. Fariselli and R. Casadio Bioinformatics **17**, 202 (2001).
- [33] M. Vendruscolo, E. Paci, C. M. Dobson and M. Karplus, Nature **409**, 641 (2001)
- [34] T. Wang, J. Miller, N. S. Wingreen, C. Tang and K. A. Dill, J. Chem. Phys., **113**, 8329 (2000).

FIGURES

FIG. 1. The contact map is a binary representation of the three-dimensional structure of the folded protein. The contact vector is constructed by summing up the rows of the contact map.

FIG. 2. Hidden surface area per residue (after appropriate scaling) vs number of contacts per residue. The histogram is obtained by averaging over 177 representative proteins with a threshold on the C_α distance between amino-acid pairs [5]. The number of occurrences is gray-scale coded, increasing from 0 to 500. The coefficient of correlation is 0.8.

FIG. 3. The native contact map (red) of protein CI2 (PDB code 2ci2) and a non-native map (blue) with the same contact vector are overlapped. For clarity, the symmetric half of the non-native contact map is omitted.

FIG. 4. Solution of the mean-field equations for the maximal and minimal degeneracy of contact vectors with finite average contact number. Maximum contact number is chosen to be 4 as for the cubic lattice. The solution for each p_i is drawn within the corresponding horizontal band. The y-axis of each band is labeled on the left and right alternatingly. For fixed average contact number, c , lowest degeneracy is when the standard deviation in the contact numbers is maximal, and vice versa.

FIG. 5. Scaling of number of contact maps and vectors with chain length, obtained by exact enumeration on the three dimensional cubic lattice. The inset (also a log-plot) shows clearly that the deviation between the two growth rates is real.

FIG. 6. Degeneracy of the contact vector on a 6×6 square. The upper graph is a log-plot of the number of distinct contact vectors with the degeneracy given on the x -axis. The lower graph shows the fraction of SAWs of size 32 and 36 inside the square, covered by the subset of corresponding contact vectors with degeneracy $\leq x$.

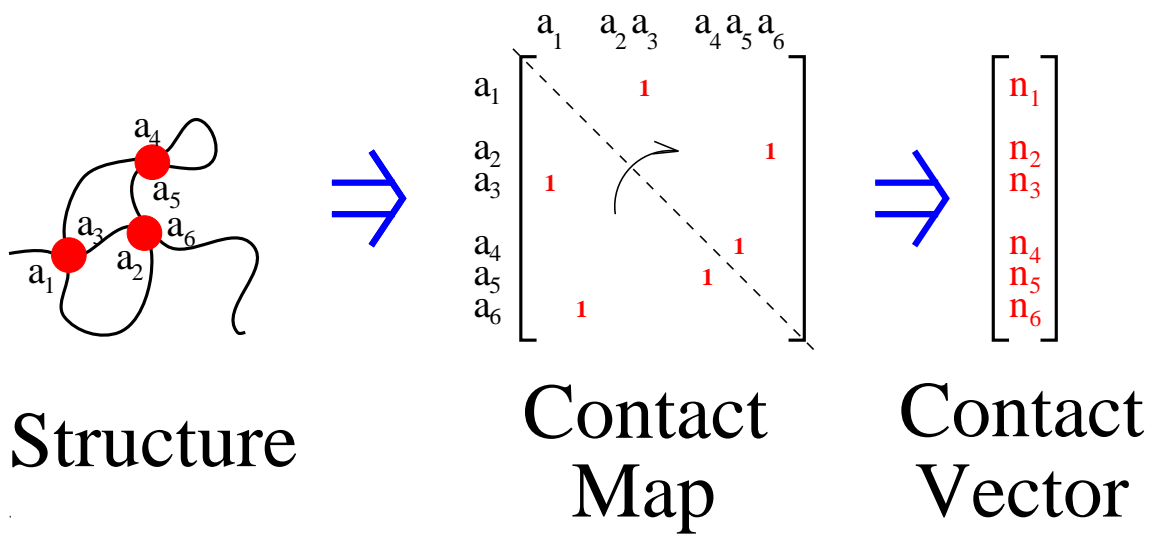


Figure 1

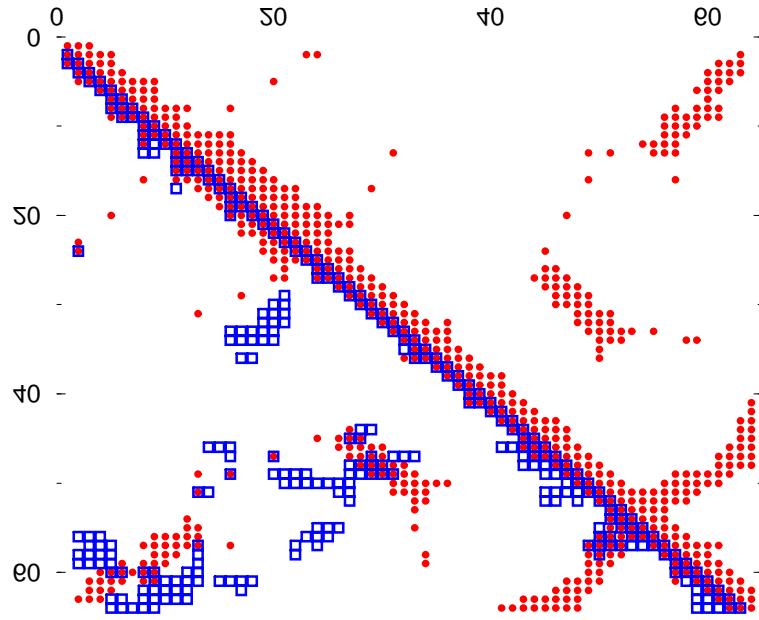


Figure 3

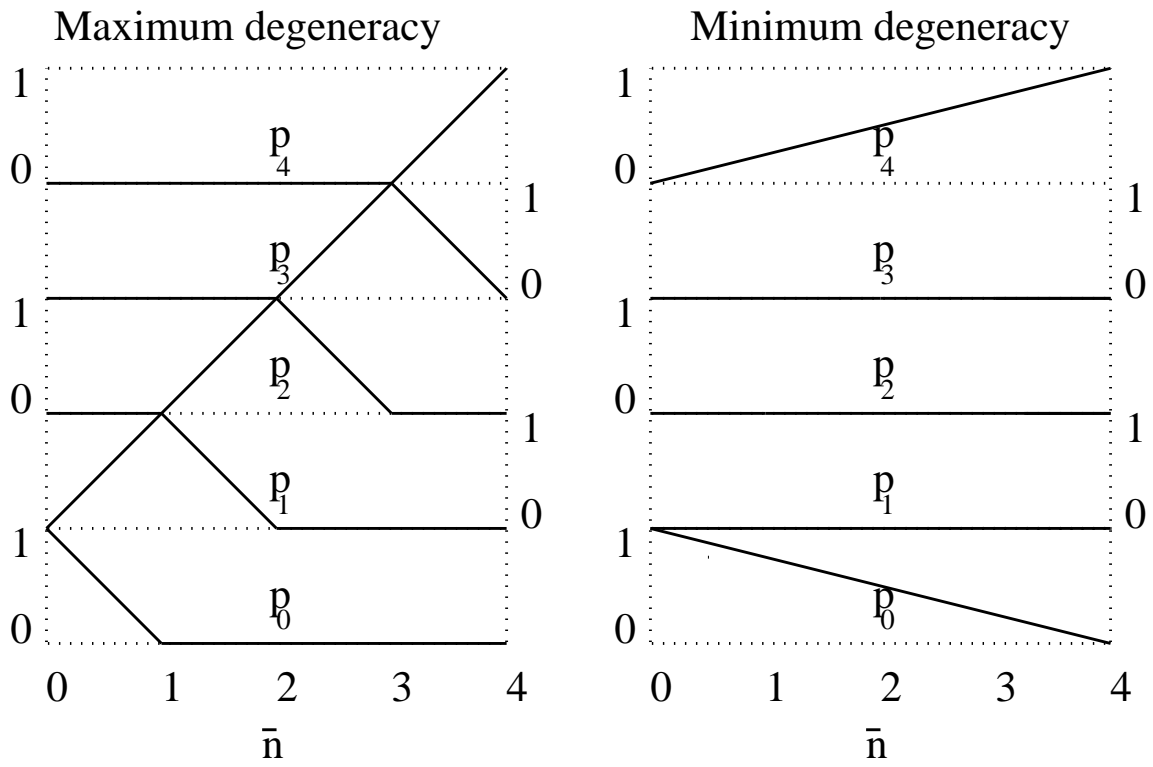


Figure 4

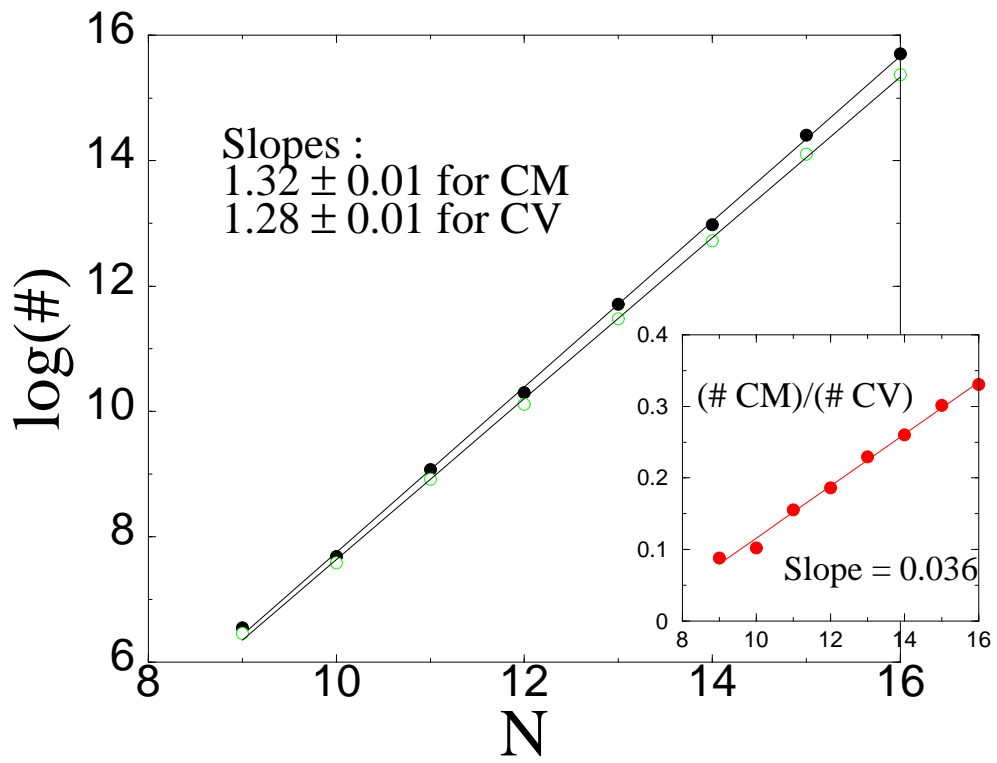


Figure 5

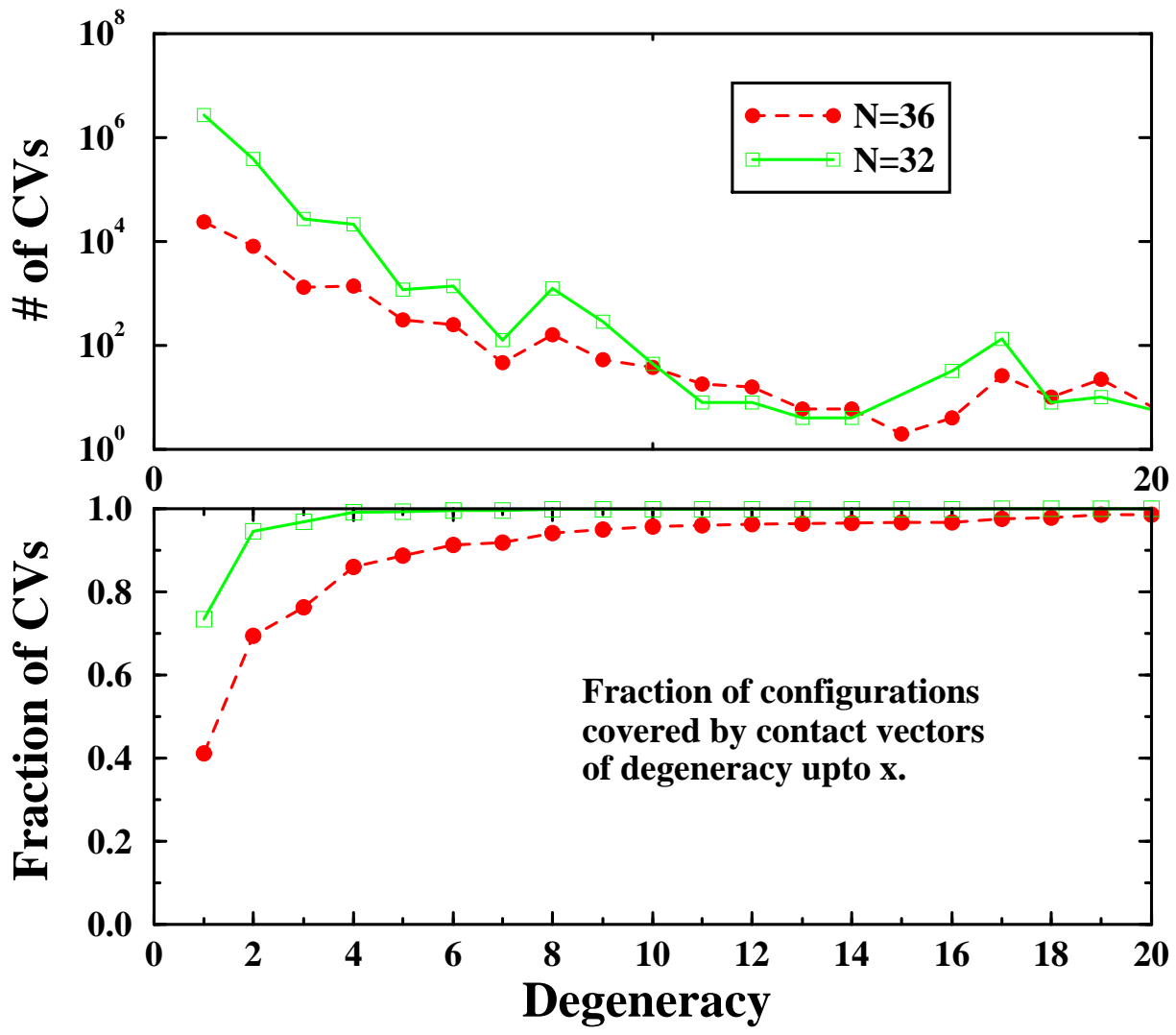


Figure 6